NEW TEORETICAL CYCLE FOR ACTIVE COMBUSTION CHAMBER ENGINE

MICHAL PIOTR GLOGOWSKI[1], PRZEMYSŁAW KUBIAK[2], ŽELJKO ŠARIĆ[3], DALIBOR BARTA[4]

Abstract

This paper presents calculations of the theoretical cycle of engines with an active combustion chamber depending on energy delivery and dissipation. In the case of ACC engines, a different calculation approach is required to account for the possibility of additional volume change, independent of the piston-crank system. The introduction presents a schematic diagram of volume change, accomplished by two independent piston-crank systems and an active combustion chamber, as proposed by the authors. Moreover, the diagram, which is the basis for analysis in this paper, illustrates characteristic points of the cycle. In existing theoretical cycles of combustion, this issue does not present any difficulties, since the solution is exact and based on known equations. In the case of theoretical ACC engines, however, the situation is different, since this engine can perform not only in typical cycles, but also in new ones. To explain the challenges of these new cycles, authors present a few of the most probable calculation variants, taking into account the new kinematic capabilities of ACC engines. Each comment justifying the choice of a certain calculation variant is illustrated with a theoretical cycle figure and closest approximation of induced pressure course of the ACC engine. At the same time, however, the authors show that this problem can have many interpretations. It has been concluded that the solution depends on the assumptions made about the active combustion chamber, namely its principle of operation.

Keywords: Theoretical Cycle, Combustion Engine, Compression Ratio, Additional Volume, Active Combustion Chamber.

Nomenclature:

$\alpha = \frac{V_5}{V_3}$ – load ratio

$\beta = \frac{p_3}{p_2} = \frac{T_3}{T_2} = \varepsilon^{(1-k)} \frac{T_3}{T_1}$ – pressure ratio

$\gamma = \frac{Q_{otto}}{Q_{max}}$ – Otto power ratio

$\varepsilon = \frac{V_1}{V_2}$ – compression ratio

$k = \frac{c_p}{c_v}$ – specific heat ratio

$\eta_1 = 1 - \frac{1}{\varepsilon^{(1-k)}}$ – Otto cycle efficiency

η_2 – proposed cycle efficiency

[1] Department of Process Equipment, Lodz University of Technology, 116 Zeromski Str., 90-924, Lodz, Polska, e-mail: michal.glogowski@p.lodz.pl

[2] Department of Vehicles and Fundamentals of Machine Design, Lodz University of Technology, 116 Zeromski Str., 90-924, Lodz, Polska, e-mail: przemyslaw.kubiak@p.lodz.pl

[3] Faculty of Transport and Traffic Sciences, University of Zagreb, Vukelićeva ul. 4, 10000, Zagreb, Croatia, e-mail: zeljko.saric@fpz.hr

[4] Faculty of Mechanical Engineering, University of Žilina, Department of Transport and Handling Machines, Univerzitná 8215/1, 010 26 Žilina, Slovak Republic, e-mail: dalibor.barta@fstroj.uniza.sk

1. Introduction

Since the creation of a four-stroke internal combustion engine in the middle of the 19th century [3,18,23], only a handful of theoretical cycles were devised. Different designs resulted in different principles of operation [9 ,14-17].

- Otto
- Sabathe
- Miller
- Diesel
- Atkinson

The theoretical cycles [7-10,12,13] listed above determine the maximum efficiency, pressure and temperature of an ideal internal combustion engine, acting as an exemplar for working engines. There are, however, some issues that are impossible to rectify in these cycles, i.e. delivering energy of a constant temperature, as in the Carnot cycle. Is it possible for an engine to realize, in the most desirable way, all theoretical cycles dependent on the load? The answer is: possibly, but such an engine would require many different energy-delivering channels. That way, it would be possible to adjust the maximum temperature and pressure, while retaining high efficiency.

Figure 1 presents the working principle of an ACC engine, which is closest to the theoretically optimal engine. For those who encounter the concept of the ACC engine for the first time, there follows a short description of its principle of operation. More detailed information on ACC engines can be found in papers related to engine research [11,19-22].

The principle of operation of an engine with an active combustion chamber, referred to as an ACC system, is as follows: the moment the pressure in the cylinder surpasses the initial pneumatic spring (3) tension, a partition wall of the ACC, which is an additional piston, ascends and stores energy in the spring (3). When the piston (2) is at the highest position, the energy stored in the spring (3) is at its highest as well. Then, all the forces acting on the piston (3), including inertia forces, are balanced out. From this moment on, during the retraction stroke of the piston, the energy stored in the spring is recuperated. Then, the additional piston (2) descends, and due to the energy stored in the spring (3), it can sustain pressure and volume in the combustion chamber at a certain, constant level. The movement of the piston (2) in every position is controlled by a one-way pneumatic spring (5) and a one-way damper (6). Adjustment of the ACC system is achieved by changing the stiffness of the pneumatic spring (3) in two ways: by altering the volume of the spring via a movable partition wall (4) and by altering the pressure supplied to the spring. Thus, the volume of the combustion chamber is dependent neither on the crank nor the piston [1,2,4-6].

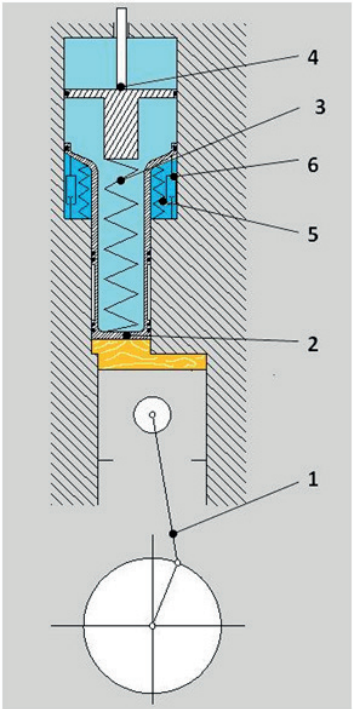

Fig. 1. Schematic diagram of ACC engine.

2. Theoretical cycle of the ACC Engine without compression ratio adjustment

Figures 2 and 3 present the working principle of a spark ignition ACC engine in its characteristic points (A, B, C, D). The position of points C (from to behind the top dead centre) and D (from to behind the top dead centre) in figure 2 are typical of the ACC system and were acquired mainly during the piston position measurement. This behaviour of the ACC system was used to devise a scheme of its working principle, seen in figures 4 and 5. The characteristic points from figures 2 and 3 (A, B, C, D) are replaced with corresponding points A', B', C' and D'.

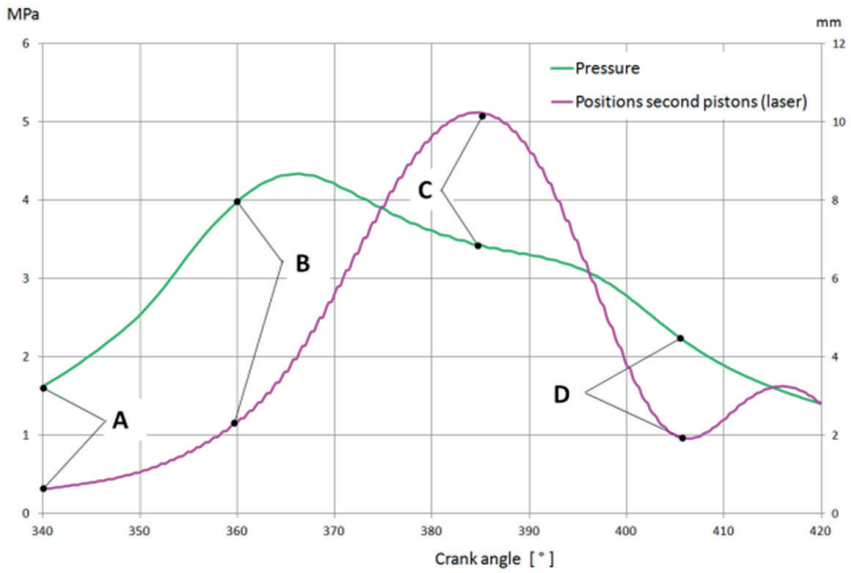

Fig. 2. Four (A, B, C, D) characteristic points of a working ACC engine for partial loads.

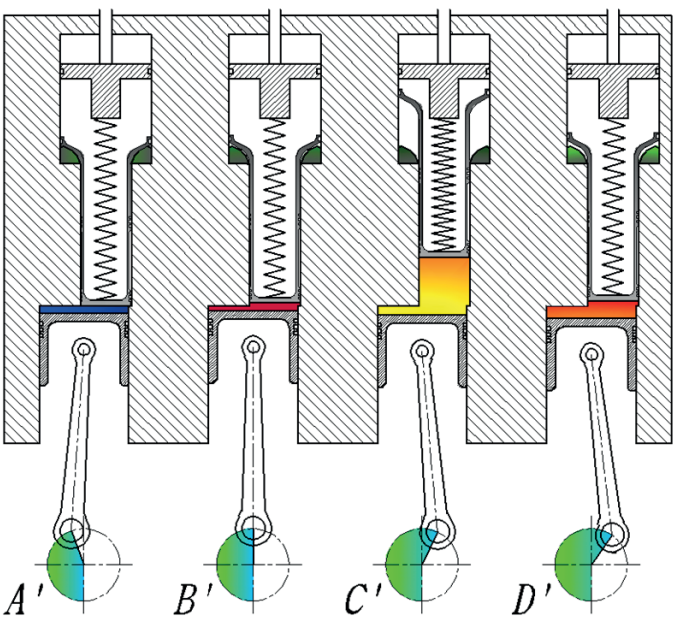

Fig. 3. Four (A, B, C, D) characteristic points of a working ACC engine.

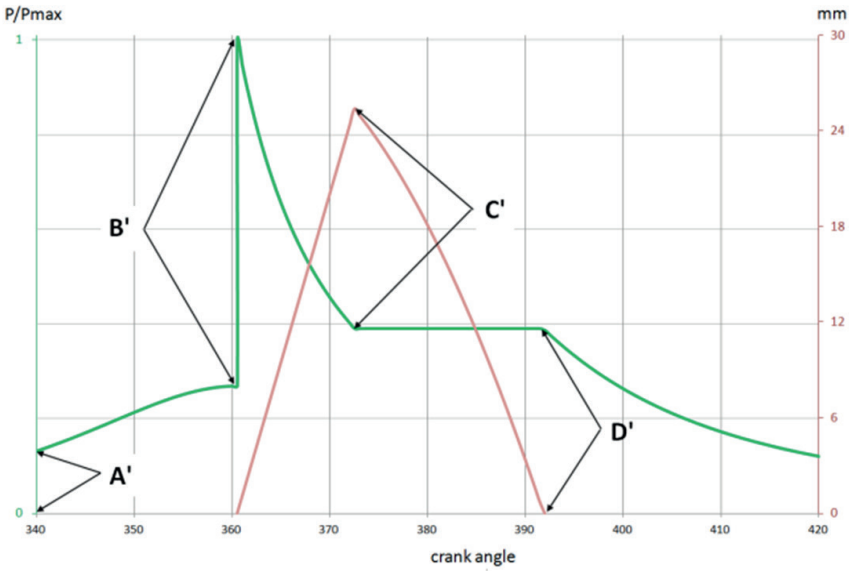

Fig. 4. Four characteristic points of a theoretical ACC engine.

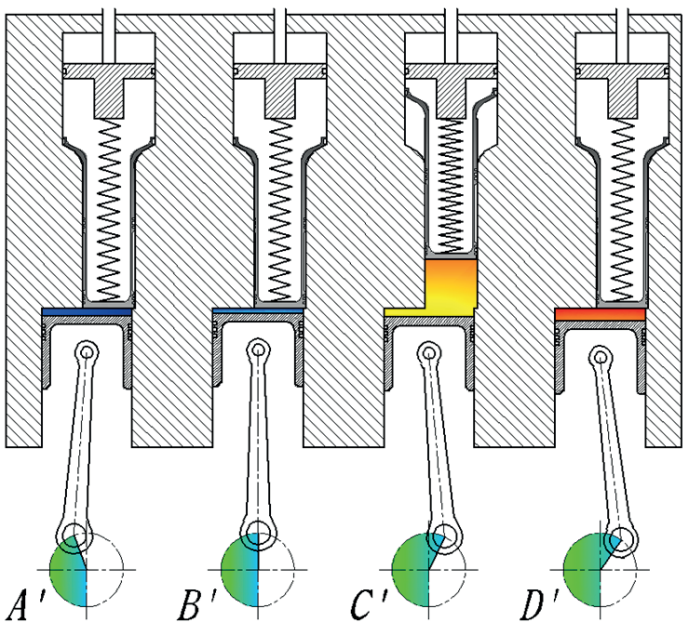

Fig. 5. Four (A, B, C, D) characteristic phases of a working ACC engine.

The ignition delay and small corresponding displacement of the ACC system in schemes in figures 4 and 5 are omitted, as standard in analyses of typical theoretical cycles.

In both schemes in figures 3 and 5, one can notice the significant influence of the ACC system, especially between points B and D for the working engine and C' and D' for the theoretical engine, that happens to be the stroke. That is why the theoretical ACC engine cycle needs a different analytical concept than in the case of the Otto cycle, which is used in analyses of subsequent VCR engine cycles. The working concept of an ACC engine according to the new cycle relates to the form of energy delivered to the system, which is presented in figure 6 with green colour and is compared with the Otto cycle, marked with red.

The concept demonstrates that when the engine is working under full load, energy should be delivered in two ways: under constant volume, marked as Q_1, as in the Otto cycle, and in a polytrophic process, marked as Q_2. When the maximum temperature criterion at maximum load has to be fulfilled, the process in which Q_2 is delivered is an isothermal process [1,15-18,23].

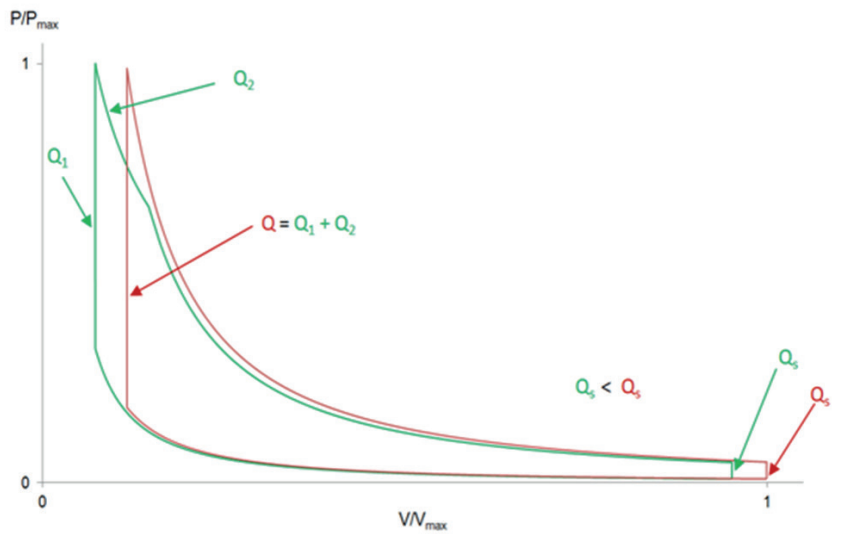

Fig. 6. Energetic concept of a new theoretical cycle. The red curve represents the Otto cycle and the green curve the ACC engine cycle.

Both cycles presented in figure 6, Otto and the new cycle, have exactly the same efficiency and maximum pressure, while retaining the maximum pressure at the same level. The most significant difference is the maximum temperature of these cycles, which is lower in the case of the ACC cycle, and will be proven by means of calculations.

3. Calculations for the new cycle

Calculations are based on the concept presented in figure 7, which is a division of the new cycle into two equal-energy cycles. The first grey-filled area is the Otto cycle with a compression ratio of 20:1, while the orange-filled area is the addition to the new cycle (according to the superposition principle).

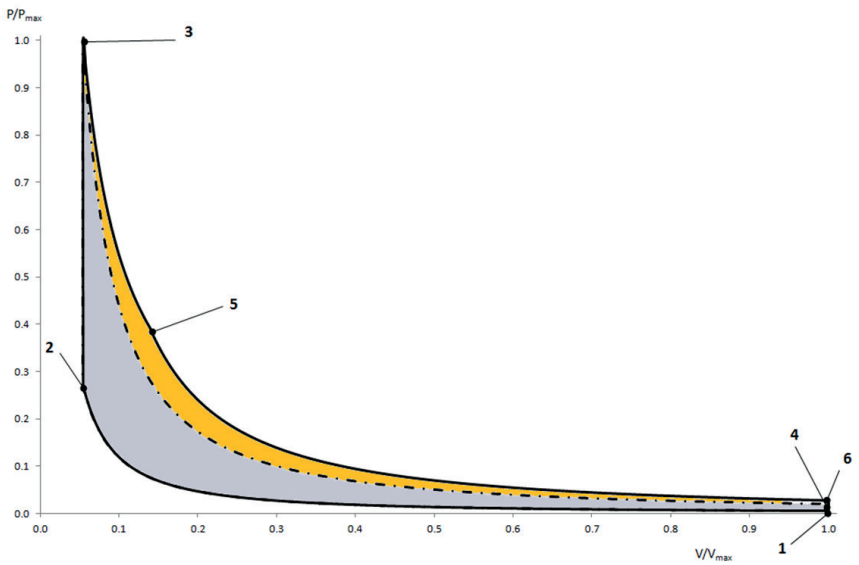

Fig. 7. The division of the new cycle.

Such division eliminates the deliberations about the apparent compression ratio change related to movement of the additional piston, that occurs during the stroke has no influence over its value. However, its effect will be accounted for by the coefficients introduced later in the paper.

In the Otto cycle (grey area) the main process occurs, which depends only on the load and fuel type, and which can range from 60% to 100% of the total energy. In the new cycle (orange area) the process of the remaining energy (0% to 40%) occurs.

This division shows that if the system does not exceed the maximum energy Q1=60% that can be delivered with the isochoric process, then the theoretical ACC engine will work with a maximum compression ratio of 20:1, according to the Otto cycle, with constant efficiency. This gives an advantage of approximately 9% of efficiency, compared to engines working under partial load with a compression ratio of 11:1. Conversely, further increase of the energy in the cycle, will also increase the contribution of the new cycle. Its efficiency will decrease by shortening the adiabatic expansion curve, finally reaching a minimum value for the isothermal process.

According to the above, one can state that when:

$$(\mathbf{Q} \leq \mathbf{Q_{1max}}) \rightarrow \eta_{\mathbf{otto}}(\mathbf{60\%}) \tag{2}$$

or

$$(\boldsymbol{\gamma} = \mathbf{1}) \rightarrow \eta_{\mathbf{otto}}(\mathbf{60\%}) \tag{3}$$

where:

$$\boldsymbol{\gamma} = \frac{\mathbf{Q_1}}{\mathbf{Q}} \tag{4}$$

However, when:

$$(\mathbf{Q_{max}} \geq \mathbf{Q} \geq \mathbf{Q_{1max}}) \rightarrow \eta_{\mathbf{prop}} = \frac{\mathbf{W_{1max}+W_2}}{\mathbf{Q}} = \frac{\eta_1\mathbf{Q_{1max}}+\eta_2\mathbf{Q_2}}{\mathbf{Q}} \tag{5}$$

or

$$(\boldsymbol{\gamma} < \mathbf{1}) \rightarrow \eta_{\mathbf{prop}} = \eta_1\boldsymbol{\gamma} + \eta_2(\mathbf{1}-\boldsymbol{\gamma}) \tag{6}$$

Assuming that in the new cycle, the process in which the remaining energy is delivered is isobaric, the following equation for the Seilger-Sabathe cycle can be formulated:

$$\eta_{\mathbf{sabathe}} = \mathbf{1} - \boldsymbol{\varepsilon}^{(\mathbf{1}-\mathbf{k})}\frac{\boldsymbol{\beta}\boldsymbol{\alpha}^{\mathbf{k}}-\mathbf{1}}{(\boldsymbol{\beta}-\mathbf{1})+\mathbf{k}\boldsymbol{\beta}(\boldsymbol{\alpha}-\mathbf{1})} \tag{7}$$

or

$$(\boldsymbol{\gamma} < \mathbf{1}) \rightarrow \eta_{\mathbf{prop}} = \eta_1\boldsymbol{\gamma} + \eta_2(\mathbf{1}-\boldsymbol{\gamma}) \tag{8}$$

where:

$$\eta_2 = \frac{\mathbf{W_2}}{\mathbf{Q_2}} = \frac{\mathbf{Q_2}-\mathbf{c_v m}(\Delta\mathbf{T_{5-6}})}{\mathbf{Q_2}} = 1 \tag{9}$$

$$\frac{\mathbf{c_p}(\mathbf{T_6}-\mathbf{T_4})}{\mathbf{c_p}(\mathbf{T_5}-\mathbf{T_3})} = 1 - \frac{\mathbf{c_p}(\mathbf{T_6}-\mathbf{T_4})}{\mathbf{k}(\mathbf{T_5}-\mathbf{T_3})} \tag{10}$$

$$\eta_2 = \mathbf{1} - \boldsymbol{\varepsilon}^{(\mathbf{1}-\mathbf{k})}\frac{(\boldsymbol{\alpha}^{\mathbf{k}}-\mathbf{1})}{\mathbf{k}(\boldsymbol{\alpha}-\mathbf{1})} \tag{11}$$

Assuming that the process in the new, additional cycle is polytrophic, the efficiency of the new cycle for an ACC engine can be formulated. Efficiency in the polytrophic process of exponent n=0.6 is presented in figure 8, marked with green colour.

$$\eta_2 = \frac{\mathbf{W_2}}{\mathbf{Q_2}} = \frac{\mathbf{Q_2}-\mathbf{c_v m}(\Delta\mathbf{T_{6-4}})}{\mathbf{Q_2}} = 1 - \frac{\mathbf{c_v}(\mathbf{T_6}-\mathbf{T_4})}{\mathbf{c_n}(\mathbf{T_5}-\mathbf{T_3})} = 1 - \frac{(\mathbf{n}-\mathbf{1})(\mathbf{T_6}-\mathbf{T_4})}{(\mathbf{n}-\boldsymbol{\kappa})(\mathbf{T_5}-\mathbf{T_3})} \tag{12}$$

$$\eta_2 = 1 - \varepsilon^{(1-\kappa)} \frac{(n-1)(\alpha^{\kappa-n}-1)}{(n-\kappa)\ \alpha^{1-n}-1} \tag{13}$$

Assuming that the process in the additional cycle in which the remaining energy is delivered is isothermal, meaning that all the energy is used for work, the efficiency of the additional cycle can be formulated as follows:

$$Q_2 = W = mRT(\ln(\alpha)) = c_v(\kappa - 1)mT_3(\ln(\alpha)) \tag{14}$$

$$\eta_2 = \frac{Q_2 - c_v m(\Delta T_{6-4})}{Q_2} = 1 - \frac{c_v m(T_6 - T_4)}{Q_2} = 1 - \frac{(T_6 - T_4)}{(\kappa-1)\ln(\alpha)} \tag{15}$$

$$\eta_2 = 1 - \varepsilon^{(1-k)} \frac{(\alpha^{\kappa-1}-1)}{(\kappa-1)\ln(\alpha)} \tag{16}$$

In these considerations the worst-case scenario of the additional cycle efficiency being equal to zero was taken into account. This is the limit of applicability, which does not occur during the ACC engine analysis. In this case, when the load is greater than 60%, efficiency will decrease gradually, as presented in figure 8 with a black dashed line.

$$\eta_2 = 0 \tag{17}$$

For the sake of calculations and plot preparation based on figures 8 and 9, the formula for the coefficient was used. Its value can be calculated assuming the values of the following parameters:

- maximum pressure or maximum temperature, $T_{max}=T_3$
- ambient temperature, $T_\alpha=T_1$
- coefficient by defining its minimum value
- compression ratio ε
- polytrophic process exponent , denoting the manner of energy delivery in the additional cycle

For the isobaric process, the following relations are true:

$$Q_2 = \left(\frac{1}{\gamma} - 1\right) Q_1 = \left(\frac{1}{\gamma} - 1\right) c_v m(T_3 - \frac{1}{\beta} T_3) \tag{18}$$

or

$$Q_2 = c_p m(T_5 - T_3) = \kappa c_v m(T_5 - T_3) \tag{19}$$

$$T_5 = (\frac{1}{\kappa})\left(\frac{1}{\gamma} - 1\right)(T_3 - \frac{1}{\beta} T_3) + T_3 \tag{20}$$

$$\alpha_{(p=const)} = \left(\frac{V_5}{V_3}\right) = \left(\frac{T_5}{T_3}\right) = (\frac{1}{\kappa})\left(\frac{1}{\gamma} - 1\right)\left(1 - \frac{1}{\beta}\right) + 1 \tag{21}$$

Heat $\mathbf{Q_2}$ can be found by means of:

$$\mathbf{Q_2} = \left(\frac{1}{\gamma} - \mathbf{1}\right) \mathbf{Q_1} = \left(\frac{1}{\gamma} - \mathbf{1}\right) \mathbf{c_v m (T_3 - T_2)} \tag{22}$$

For the polytrophic process, the following relations are true:

$$\mathbf{Q_2} = \mathbf{c_n m (T_5 - T_3)} = \frac{\mathbf{(n-1)}}{\mathbf{(n-\kappa)}} \mathbf{c_v m (T_5 - T_3)} \tag{23}$$

$$\mathbf{T_5} = \frac{\mathbf{(n-1)}}{\mathbf{(n-\kappa)}} \left(\mathbf{1} - \frac{\mathbf{1}}{\gamma}\right) \mathbf{(T_3 - T_2)} + \mathbf{T_3} \tag{24}$$

$$\boldsymbol{\alpha}_{\mathbf{(n=const)}} = \left(\frac{\mathbf{V_5}}{\mathbf{V_3}}\right) = \left(\frac{\mathbf{T_5}}{\mathbf{T_3}}\right)^{\left(\frac{\mathbf{1}}{\mathbf{n-1}}\right)} = \left[\frac{\mathbf{(n-1)}}{\mathbf{(n-\kappa)}} \left(\frac{\mathbf{1}}{\gamma} - \mathbf{1}\right) \left(\mathbf{1} - \frac{\mathbf{1}}{\boldsymbol{\beta}}\right) + \mathbf{1}\right]^{\left(\frac{\mathbf{1}}{\mathbf{n-1}}\right)} \tag{25}$$

For the isothermal process, the following relations are true:

$$\mathbf{Q_2} = \mathbf{(\kappa - 1)\, c_v m T_3 (ln(\alpha))} \tag{26}$$

$$\boldsymbol{\alpha}_{\mathbf{(T=const)}} = \left(\frac{\mathbf{V_5}}{\mathbf{V_3}}\right) = \mathbf{e}^{\left[\left(\frac{\mathbf{1}}{\boldsymbol{\kappa-1}}\right)\left(\frac{\mathbf{1}}{\gamma}-\mathbf{1}\right)\left(\mathbf{1}-\frac{\mathbf{1}}{\boldsymbol{\beta}}\right)\right]} \tag{27}$$

Based on the performed calculations, a graph in figure 8 with α, β and γ coefficients and a graph in figure 9 with the ACC engine cycle efficiency for four coefficient values n, were plotted. The values are 0.0, 0.5, 0.8 and 1.0.

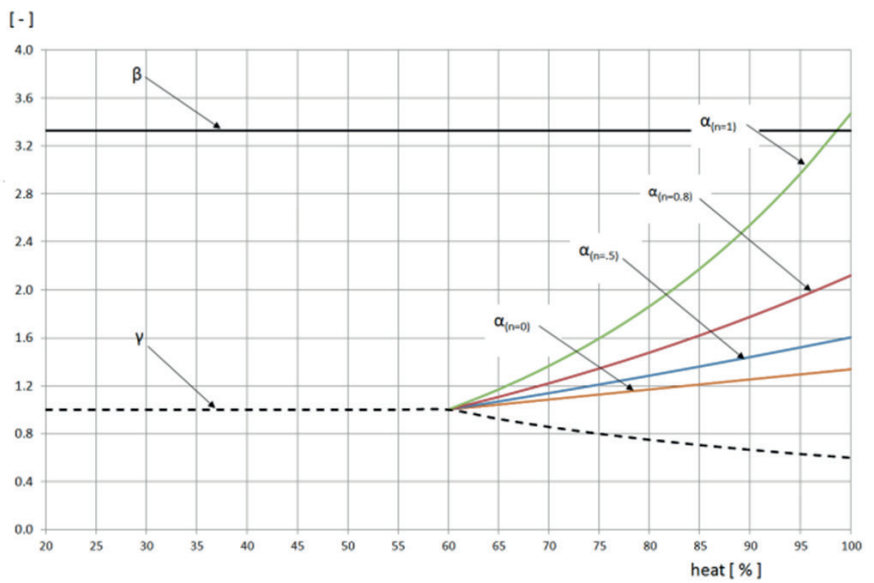

Fig. 8. α, β, γ coefficients as a function of load.

As anticipated, as the polytrophic exponent n increases, the coefficient increases as well. This is accompanied by a decrease in the additional cycle efficiency. The larger $n2$ is, the smaller the coefficient is.

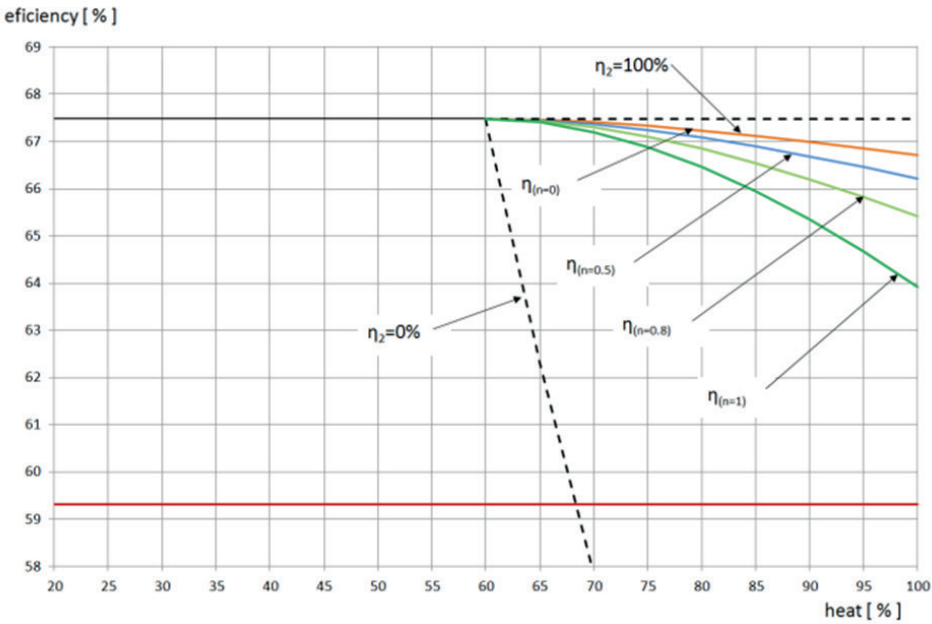

Fig. 9. Efficiency of the new Otto cycle as a function of load.

Figure 9 shows that the lowest efficiency at full load occurs in the ACC cycle where the energy Q2 is supplied in isothermal process. Decreasing efficiency, i.e. increasing polytrophic exponential n, is accompanied by a drop of maximum temperature, which is shown in Figure 11.

It should be noted that plots in Figure 10 were produced for full load, in order to show the maximum temperature differences and not to dwell upon the lambda coefficient. Following assumptions were made to produce these plots:

- comparable cycles have the same swept volume,
- reference temperature is the maximum temperature of Otto cycle with compression ratio 11:1,
- for all cycles, to simplify the calculations the cp/cv=1.75 (whereas in a real engine it is between 1.28 and 1.38 what was accounted for in simulation in),
- the value of λ=1 (the lambda of stoichiometric mixture) for theoretical ACC engine and $\sim\lambda$=1.05 for engine working according to Otto cycles with compression ratio 11:1, which stems from the different combustion chamber volumes,

- all calculations were conducted relative to overall volume,
- in each case, the system was supplied with the same amount of energy,
- in case of theoretical ACC engine, the energy is returned in isochoric process, thus the overall volume of system does not change.

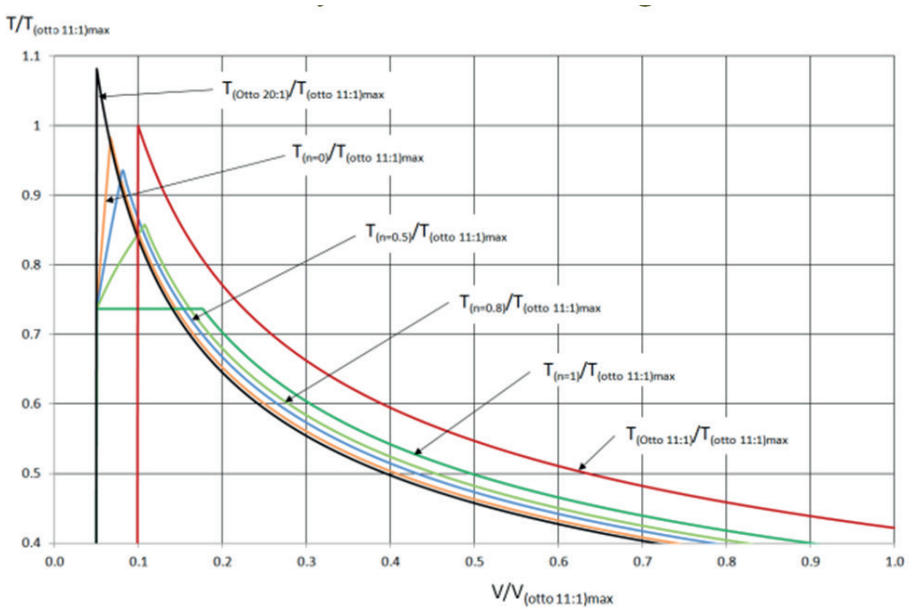

Fig. 10. Relative temperature of Otto and the new cycle for different polytrophic exponents.

Taking such assumptions, the effect of ACC system on theoretical cycle in Figures 6, 7 and 10 is not visible. Therefore, this paper includes Figures 12 and 13, scaled down to the volume of crank piston system, as well as Figure 13 and 14 (theoretical and real) scaled with reference to crankshaft angle. These plots enable the assessment of correlations between the theoretical and real ACC engine cycle.

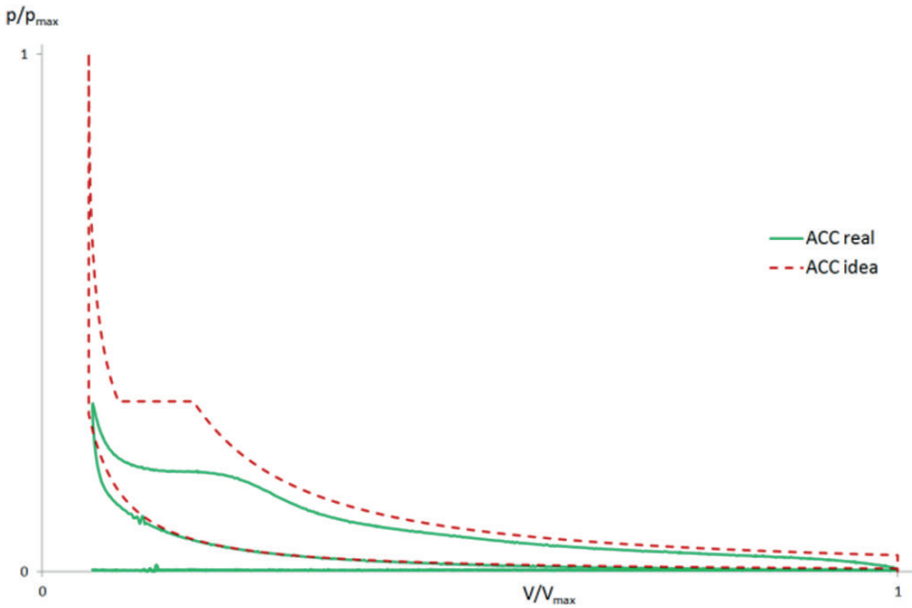

Fig. 11. Course of pressure as a function of relative volume of crank piston system in real and theoretical engine.

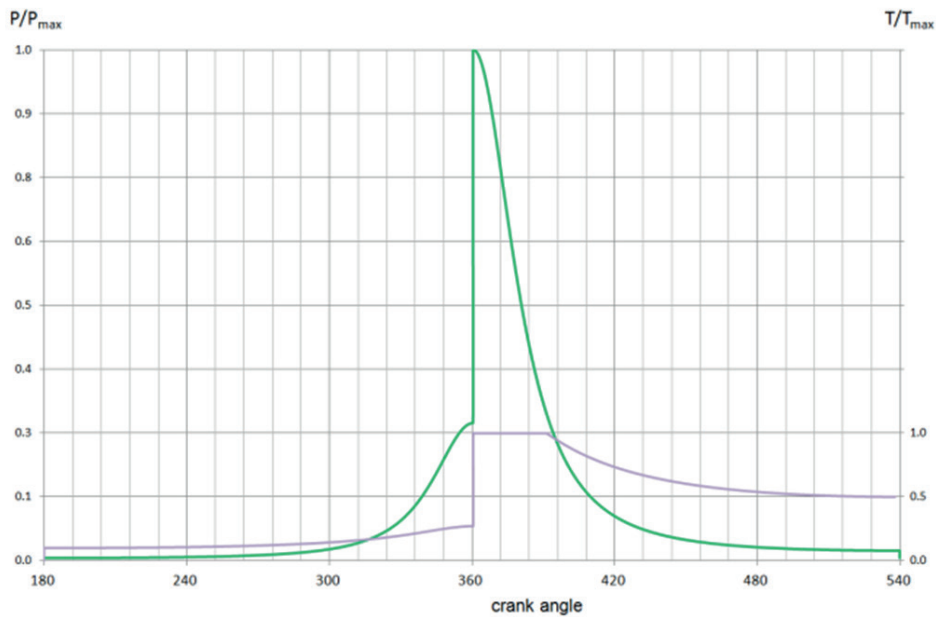

Fig. 12. Course of pressure and temperature as a function of crank angle in real and theoretical engine.

The plot in figure 12 needs additional backing with experimental measurements that was the basis for recreation of temperature course in the chamber of real engine. The aim in this case was to prove that combustion reaction occurs in constant temperature, which should limit the discussions about the possibility of isothermal theoretical cycle. Such plot is presented in figure 13, where temperature is constant for the period of time that is significant for the process. Despite the distortions of the pressure that stem from the heat transfer, there are no combustion in the specific temperature.

In Figure 13 the course of temperature was replaced with measurement results of the radiant intensity from the real ACC engine. The measured photoelectric effect is a function of temperature of fourth power, according to Stefan-Boltzmann law. This illustrates well the change of temperature in the cylinder, even if the devices were not rated, as in this case.

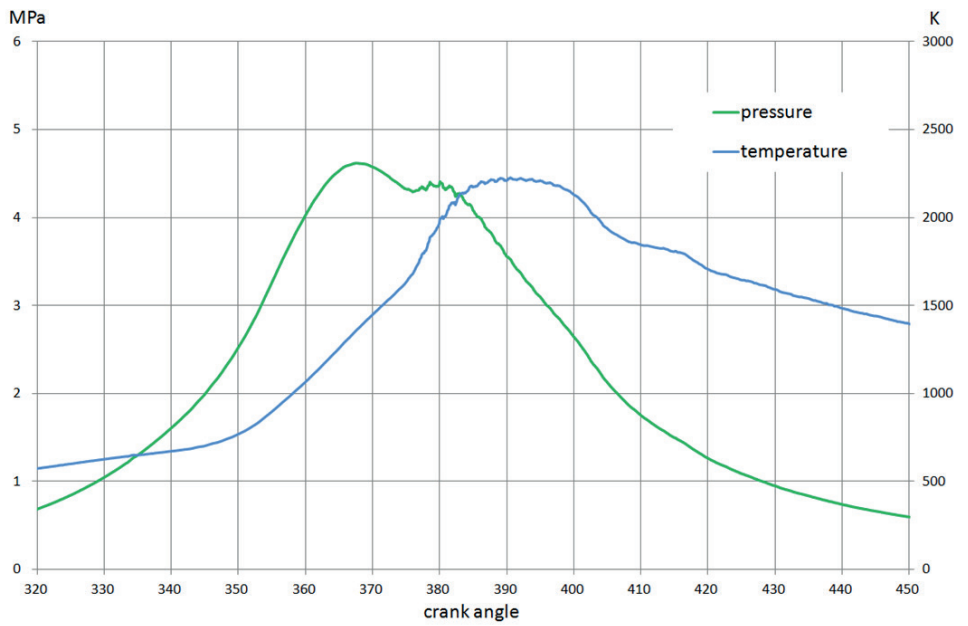

Fig. 13. Course of pressure and temperature in real ACC engine as a function of crank angle.

The figure 14 presents the correlation between volume change dV and temperature. Its purpose is to demonstrate the direct influence of ACC system on the course of temperature in ACC engine chamber. The volume change is measured by means of a laser transducer.

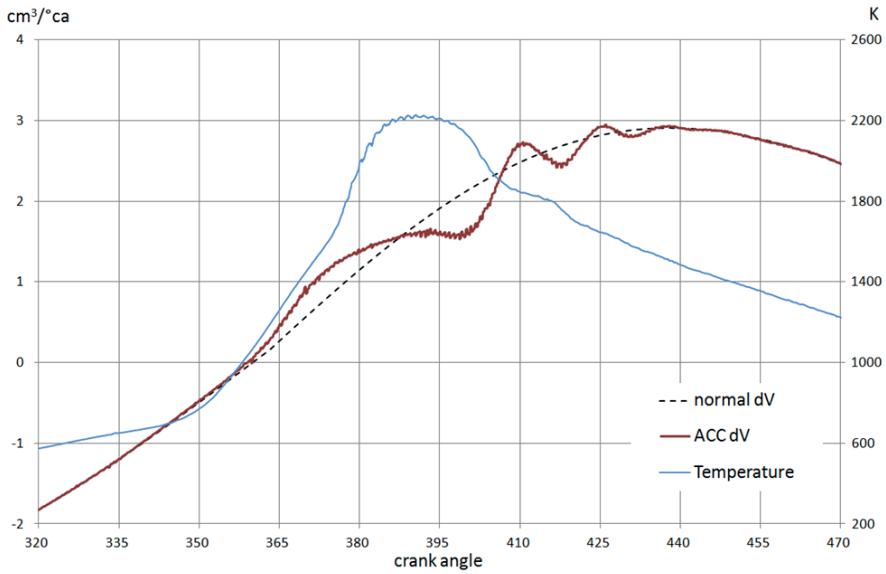

Fig. 14. Course of temperature and volume change in real engine as a function of crank angle.

Concluding the preceding calculations concerning the new proposed theoretical cycle, it is important to underline that the ACC system introduces additional loss, when the exponent of the polytrophic process is greater than 0, $n\rangle 0$. This means that energy is accumulated at higher pressure and recuperated at lower pressure, as illustrated by the arrow in figure 15.

The yellow area, marked as "+" depicts the energy accumulation area, whereas the blue area, marked with "-" depicts energy recuperation. The difference in this closed indicator diagram is equivalent to the efficiency of an ACC system and, in this case, it is equal to η_{ACC}=67%.

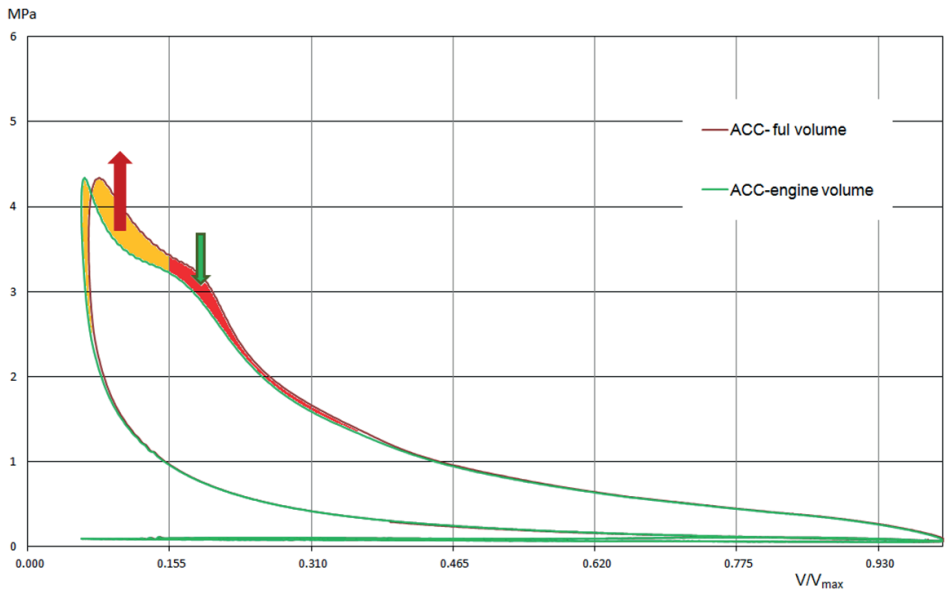

Fig. 15. Real energy balance of an ACC system for a closed cycle.

In both real and theoretical cycles, energy gradually lost due to the recuperation process is related to an increase in kinetic energy.

In the working cycle, energy will be lost mainly due to kinetic energy gain and the overcoming of friction. The value of lost energy, calculated for the whole cycle, varies between 0% and 7%, depending on the maximum cycle temperature and load. The working cycle is characterised by an increase in insignificant loss, which in some cases may even decrease. The loss is calculated as the difference between accumulated and recuperated energy in a working cycle, and is of a value between 55% and 80%.

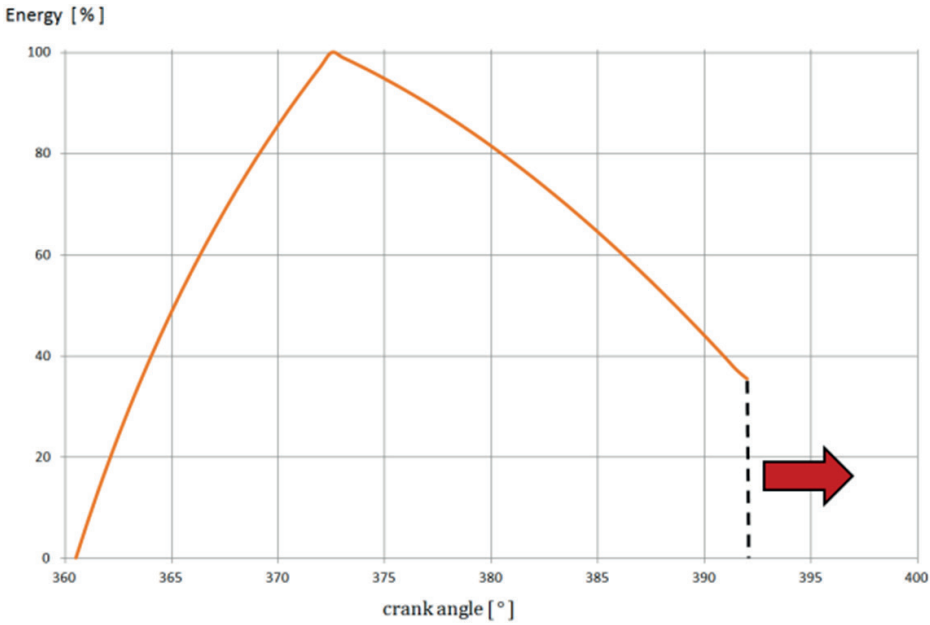

Fig. 16. Course of accumulation and recuperation of energy in a theoretical (frictionless) ACC system.

In the face of these losses, the theoretical cycles should be modified into a form that would produce more accurate calculations. Such a form is presented in figure 16. The process of losing additional energy by the ACC system is assumed to be isochoric.

Such energy recuperation in ACC system was observed when engine speed was below 2000 rpm. In this case, the pressure in the cylinder was constant for a period of time. This was possible due to the volume change compensation of the piston-crank system by the ACC system.

Unfortunately, another phenomenon occurred at higher speeds, which required additional modifications of the cycle. That is why the authors ceased calculations and presented the ACC system as synchronized and loss-free.

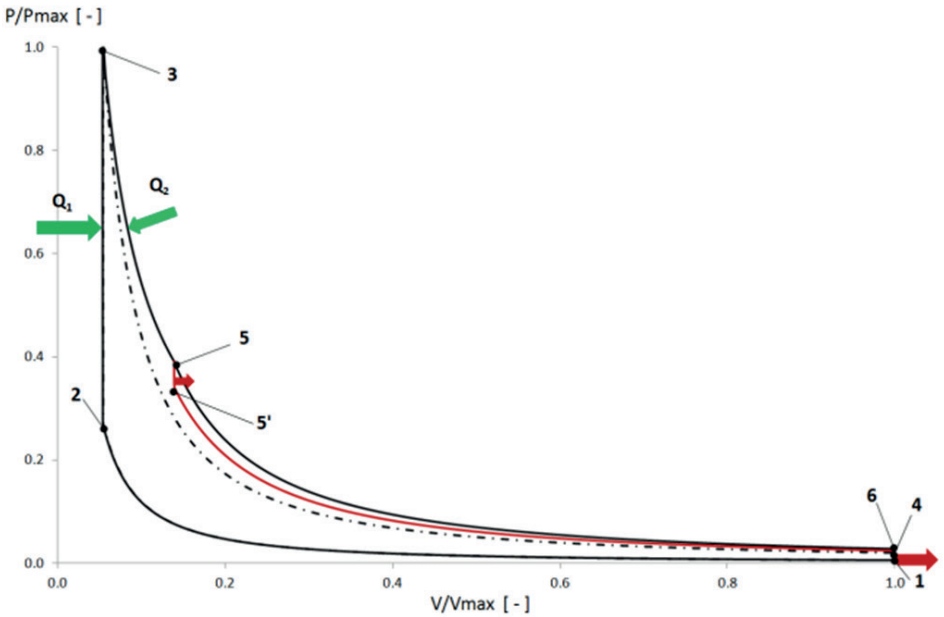

Fig. 17. Theoretical cycle of an ACC engine that includes losses in ACC cycle.

4. Recapitulation and conclusions

Without a doubt, the additional kinematic system called active combustion chamber, taking part in the shaping of the theoretical cycle, presents new possibilities, unavailable in other kinematic systems. The analysis performed makes assumptions about the behaviour of ACC systems, which significantly limits their capability to produce further theoretical cycles. The authors, however, deem these cycles as most energy-efficient and closest to actual working ACC engine cycles, what is well shown in Figure 12, 14 and 15.

The fundamental conclusions that can be drawn from the presented analysis are:

1. The efficiency of a theoretical ACC engine is directly dependent on the kinematic system that works on surroundings, which in the case of internal combustion piston engines is usually the piston-crank system. Therefore, all action leading to efficiency increase in a theoretical ACC engine should be carried out in regard to work done on surroundings.
2. The ACC system, which on principle produces losses, has only one purpose: to balance energy by doing work in order to get the desired results. Its losses stem from absorbing energy at higher pressures and releasing energy at lower, but not in the case of the isobaric process. Energy in this system should be transferred in the right moment,

in order to maintain the balancing process, which denotes the difference between the accumulation and recuperation processes.

3. It is beneficial for the system, when the efficiency of the energy-balancing process is at least as high as that in the Otto cycle, to correspond to the maximum compression ratio of a theoretical ACC engine. Otherwise, the efficiency of the whole cycle decreases significantly.
4. On principle, the ACC system enables the adjustment of temperature and pressure during energy delivery to the cycle, specifically in the final phase.
5. The ACC system presented in the calculations is deprived of friction; therefore, its lost energy should be interpreted as the kinetic energy of the system. This energy in a working engine is dissipated in damped vibrations.
6. Both theoretical and working ACC engines are characterised by lower temperature at the end of the expansion process (stroke). This stems from earlier than in comparable cycles energy dissipation by the ACC system. It occurs during energy recuperation and influences the maximum cycle temperature.
7. This analysis omits cases where the ACC system not only balances the energy, but also adjusts the compression ratio. In these cases, additional calculation variants are introduced, which supersedes the scope of this research paper. It is worth researching the cases when the ACC system's efficiency is higher than that presented in this paper. This is primarily connected to the fact that energy accumulation starts at lower pressure, and pressure adjusts the compression ratio. The authors will attempt to consider these cases and illustrate them with pressure diagrams for working ACC engines in future papers.
8. In this paper, the energy recuperation problem was omitted, as no precise solution was found. This relates mainly to the undefined way of energy dissipation, meaning the difference between the energy that returns to the cycle and that which is lost.

References

[1] Alkidas AC. Heat Transfer Characteristics of a Spark-Ignition Engine. ASME. J. Heat Transfer. 1980;102(2):189-193., doi:10.1115/1.3244258.

[2] Angulo-Brown F, Fernandez-Betanzos J, Diaz-Pico CA. Compression ratio of an optimized air standard Otto-cycle model. (1994) European Journal of Physics, 15 (1), art. no. 007, pp. 38-42., doi: 10.1088/0143-0807/15/1/007.

[3] Beale WT, inventor; Sunpower, Inc., assignee. Free piston internal combustion engine. United States patent US 6,170,442. 2001 Jan 9.

[4] Chen L, Wu C, Sun F, Cao S. Heat transfer effects on the network output and efficiency characteristics for an air-standard Otto cycle. (1998) Energy Conversion and Management, 39 (7), pp. 643-648,. doi: 10.1016/S0196-8904(97)10003-6.

[5] Colton, R. J. Automatic booster piston for internal combustion engines. U.S. Patent 2,914,047, issued 1959, Nov 24.

[6] Dabrowski A, Glogowski M, Kubiak P. Improving the efficiency of four-stroke engine with use of the pneumatic energy accumulator-simulations and examination. International Journal of Automotive Technology. (2016) Aug 1;17(4):581-90., doi: 10.1007/s12239-016-0058-1.

[7] Douaud AM, Eyzat P. Four-octane-number method for predicting the anti-knock behavior of fuels and engines. (1978) SAE Technical Papers., doi: 10.4271/780080.

[8] Fukuzawa Y, Shimoda H, Kakuhama Y, Endo H, Tanaka K. Development of high efficiency Miller cycle gas engine. (2001) Technical Review - Mitsubishi Heavy Industries, 38 (3), pp. 146-150.

[9] Ge Y, Chen L, Sun F, Wu C. Performance of an Atkinson cycle with heat transfer, friction and variable specific-heats of the working fluid. Applied Energy. 2006 Nov 30;83(11):1210-21. Doi:10.1016/j.apenergy.2005.12.003

[10] Ghojel JI. Review of the development and applications of the Wiebe function: a tribute to the contribution of Ivan Wiebe to engine research. (2010) International Journal of Engine Research, 11 (4), pp. 297-312.,doi: 10.1243/14680874JER06510.

[11] Guy E, inventor; Guy, Evan, assignee. Fuel tolerant combustion engine with reduced knock sensitivity. United States patent US 5,476,072. 1995 Dec 19.

[12] Haraldsson G, Tunestål P, Johansson B, Hyvönen J. HCCI combustion phasing in a multi cylinder engine using variable compression ratio. SAE Technical Paper; 2002 Oct 21., doi: 10.4271/2002-01-2858.

[13] Haraldsson G, Tunestål P, Johansson B, Hyvönen J. HCCI combustion phasing with closed-loop combustion control using variable compression ratio in a multi cylinder engine. SAE Technical Paper; 2003 May 19., doi: 10.4271/2003-01-1830.

[14] Heywood J. Internal combustion engine fundamentals. McGraw-Hill Education; 1988 Apr 1.

[15] Hoffmann KH, Watowich SJ, Berry RS. Optimal paths for thermodynamic systems: the ideal Diesel cycle. Journal of Applied Physics. 1985 Sep 15;58(6):2125-34. Doi: 10.1063/1.335977

[16] Howard, G.E. Internal Combustion Motor. U.S. Patent No. 2,419,450. Issued 1947, Apr 22.

[17] Kanesaka H, inventor; Usui Kokusai Sangyo Kaisha, Ltd., assignee. Otto-cycle engine. United States patent US 5,123,388. 1992 Jun 23.

[18] Kirke, and Others Improvements in internal combustion engines. GB190827740A. 1908.

[19] Sabathe LG, inventor. Internal-combustion engine. United States patent US 883,240. 1908 Mar 31.

[20] Shadloo MS, Poultangari R, Jamalabadi MA, Rashidi MM. A new and efficient mechanism for spark ignition engines, (2015) Energy Conversion and Management, 96, art. no. 6984, pp. 418-429., doi: 10.1016/j.enconman.2015.03.017.

[21] Turner JW, Blundell DW, Pearson RJ, Patel R, Larkman DB, Burke P, Richardson S, Green NM, Brewster S, Kenny RG, Kee RJ. Project omnivore: a variable compression ratio ATAC 2-stroke engine for Ultra-wide-range HCCI operation on a variety of fuels. (2010) SAE International Journal of Engines, 3 (1), pp. 938-955., doi: 10.4271/2010-01-1249.

[22] William, T. (1997). Beale Free piston internal combustion engine. U.S. Patent No 6170442 B1.

[23] Woschni G. A universally applicable equation for the instantaneous heat transfer coefficient in the internal combustion engine. SAE Technical paper; 1967 Feb 1., doi: 10.4271/670931.